Non-destructive classification of sugarcane milling feasibility using deep learning: A comparative study of VGG19 and ResNet50

Nur Indrianti [a,1,*], Raden Achmad Chairdino Leuveano [a,2], Heru Cahya Rustamaji [b,3], Andrey Ferriyan [b,4], Panut Mulyono [c,5], Bayu Prasetya Wijaya [b,6]

[a] Department of Industrial Engineering, Faculty of Industrial Engineering, Universitas Pembangunan Nasional Veteran Yogyakarta, Indonesia
[b] Department of Informatics, Faculty of Industrial Engineering, Universitas Pembangunan Nasional Veteran Yogyakarta, Indonesia
[c] Department of Chemical Engineering, Faculty of Engineering, Universitas Gadjah Mada, Indonesia
[1] n.indrianti@upnyk.ac.id; [2] raden.achmad@upnyk.ac.id; [3] herucr@upnyk.ac.id; [4] andrey.f@upnyk.ac.id; [5] pmulyono@ugm.ac.id;
[6] bayuprasetyawijaya671@gmail.com
* corresponding author

ARTICLE INFO

Article history
Received September 28, 2025
Revised November 25, 2025
Accepted November 26, 2025
Available online February 28, 2026

Keywords
Sugarcane quality
Machine learning
Brix
VGG19
ResNet50

ABSTRACT

Assessing sugarcane quality is crucial for ensuring both economic value and processing efficiency in sugar production. Conventional approaches, such as refractometer-based Brix measurements, are destructive, labor-intensive, and unsuitable for large-scale or rapid field evaluations. This study proposes a non-destructive deep learning framework for classifying sugarcane internodes into two quality categories (< 16 °Bx and ≥16 °Bx) to address existing limitations. Two convolutional neural network architectures, VGG19 and ResNet50, were evaluated utilizing a defined transfer learning and data augmentation methodology. Because of its residual connections, which enable deeper and more stable feature learning, ResNet50 consistently outperformed VGG19, achieving the highest accuracy of 78.85% on the Luar2_Putih dataset. This comparative finding demonstrates that modern residual-based networks provide superior robustness for subtle visual classification tasks in agricultural imaging, while also validating the stability of the proposed two-phase training framework. The study advances AI-driven non-destructive quality assessment by offering a scalable, field-deployable solution that supports sustainable, efficient sugarcane processing in line with the UN Sustainable Development Goals (SDG 2, 9, and 12).

1. Introduction

Sugar is among the most extensively consumed commodities worldwide, serving as a critical input for the food, beverage, and industrial sectors [1]. Sugarcane, as its primary source, is vital not only for economic value but also as a feedstock for bioethanol, supporting sustainable energy [2]. In Indonesia, sugarcane underpins national food and energy security, with Regulation No. 40 of 2023 targeting sugar self-sufficiency by 2028 and 1.2 billion liters of bioethanol by the year 2030 [3], [4]. Achieving these targets directly supports SDG 2, SDG 7, SDG 9, SDG 12, and SDG 13 [5]. However, rapid and accurate methods for classifying sugarcane quality are urgently needed to achieve these goals.

Accurate sugarcane quality assessment is critical but remains challenging. Current industrial methods, such as destructive laboratory measurements like Brix, pol, and purity using refractometers [6], are labor-

intensive, slow, and impractical for rapid field assessment. Delays after harvest expose stalks to microbial degradation, leading to lower sucrose recovery and economic losses [7]. Although non-destructive techniques such as near-infrared (NIR) spectroscopy show promise, they require expensive lab-grade equipment and are rarely viable in the field [8]. This underscores the urgent need for affordable, scalable, non-destructive solutions for field-level quality evaluation.

Recent advancements in artificial intelligence (AI) and deep learning (DL) have influenced precision agriculture. Crop monitoring, yield forecasting, and disease identification are all aided by machine learning [9]–[11]. In sugarcane, AI-based imaging supports growth monitoring [12], disease detection [13]–[15], and yield estimation via UAV or satellite imagery [16]–[18]. Yet most studies focus on leaf- or canopy-level features rather than on direct post-harvest quality assessment at the internode level. The Brix value, which represents soluble solids and sucrose concentration, is a key indicator of sugarcane maturity and milling efficiency [19]–[21]. Developing a non-destructive, image-based system for predicting internode Brix remains a critical, underexplored direction.

Deep learning has shown strong performance in agricultural imaging, including plant disease detection [22]–[25], fruit grading [26], yield estimation [27], and morphological classification [28]. Convolutional Neural Networks (CNNs) effectively handle tasks needing fine-grained texture and color analysis [27], [29], [30]. VGG19 offers a classical, interpretable baseline, while ResNet50 uses residual connections for deeper, more stable learning. Their complementary strengths are useful for comparative evaluation in sugarcane quality assessment using Brix values. Testing VGG19 and ResNet50 under the same conditions benchmarks conventional and modern CNNs, offering insight into their relative accuracy and efficiency in real field scenarios.

Lightweight models like MobileNet, EfficientNet-Lite, and transformer-based Vision Transformers (ViTs) [31] have shown promise in agriculture. ViTs need larger annotated datasets and more resources, while lightweight CNNs are best explored after a baseline is set. Thus, this study uses VGG19 and ResNet50 to gauge internode-level Brix classification difficulty and establish a benchmark for future work on lightweight or transformer architectures.

A synthesis of prior studies Table 1 makes clear that most agricultural imaging research focuses on leaf diseases [13], [32], [33], weed detection [34], growth monitoring [12], yield prediction [27], [17], [35], [18], and variety classification [28]. Few address non-destructive quality assessment in sugarcane using internode imaging or connect image features to biochemical markers such as Brix. This reveals an explicit research gap: a lack of reproducible datasets and benchmarks for internode-level Brix classification of RGB imagery using modern deep learning.

This paper presents a non-destructive, image-based system for determining the quality of sugarcane internodes by RGB photography and deep learning to fill this gap. The objectives are as follows:

- to construct a labeled dataset pairing internode images with measured Brix values;
- to conduct a controlled comparison of two widely used CNN backbones, VGG19 and ResNet50, under standardized preprocessing, augmentation, and transfer-learning configurations; and
- to establish a transparent and reproducible baseline for intelligent sugarcane quality assessment that future research can extend using lightweight architectures, multimodal sensing, or continuous Brix prediction.

Based on this gap, the study is guided by the following research questions:

- RQ1 — Can standard CNN backbones (VGG19 and ResNet50) reliably classify sugarcane internodes into Brix-based quality categories under field-induced variability?
- RQ2 — Which combination of backbone architecture (VGG19 vs. ResNet50) and imaging configuration (Luar1/Luar2; white/black background) provides the best balance between accuracy, class-wise F1-score, and suitability for near-real-time use?

- RQ3 — To what extent can RGB-based visual cues of internode appearance serve as proxies for internal Brix, as reflected by patterns in the performance of both models across different imaging setups?.

The remainder of this paper presents the research methodology, experimental results, discussion of findings and implications, and concluding insights.

Table 1. Summary of prior studies and identified research gap

Authors	Crop / Focus	Methodology	Dataset	Key Findings	Limitation / Gap
Too *et al.* [36]	Multi-crop, plant disease	CNN (VGG16, ResNet50/101/152, DenseNet121, InceptionV4)	PlantVillage (14 crops, 38 classes)	DenseNet achieved 99.75% accuracy	Focused on leaf disease, not stalk quality
Ismail & Malik [26]	Fruit grading (apple, banana)	CNN (ResNet, DenseNet, MobileNetV2, NASNet, EfficientNet) + Ensemble	Apple & banana datasets	EfficientNet achieved 99.2% accuracy	Focus on fruits, not sugarcane
Chen *et al.* [37]	Rice leaf disease	Transfer learning (VGGNet, Inception)	Rice plant leaf dataset	Achieved 92% accuracy even under complex backgrounds	Not focused on sugarcane maturity
Zhao *et al.* [38]	Bale detection, precision agriculture	UAV + DA (Domain Adaptation)	UAV crop images (243 images)	mAP improved from 0.70 to 0.94 with DA	Object detection only, not crop quality
Canata *et al.* [17]	Sugarcane yield mapping	RF, MLR with Sentinel-2	Sentinel-2 imagery (2 cropping seasons)	RF achieved RMSE 4.63 Mg ha–1, R^2 = 0.70	Yield estimation, not internode Brix
Amarasingam *et al.* [13]	Sugarcane disease (WLD)	UAV RGB + DL (YOLOv5, YOLOR, DETR, Faster R-CNN)	UAV images from the Sri Lanka plantation	YOLOv5 achieved 95% precision	Limited to disease detection
Huang *et al.* [14]	Sugarcane disease (complex background)	DeepLabV3+, MobileNetV3, DCGAN augmentation	Custom sugarcane leaf dataset	Accuracy improved from 53.5% to 99%	Focus on leaves, not stalk maturity
Kai *et al.* [28]	Sugarcane variety classification	DNN, SVM, RF, kNN	Sentinel-2 multispectral imagery	SVM achieved 99.55% accuracy	Limited to variety classification
Maheswari *et al.* [39]	Tomato yield estimation	SegNet (VGG19, VGG16, U-Net)	Tomato field images (672 images)	VGG19-based SegNet achieved the best localization	Not sugarcane-related
Veeragandham & Santhi [34]	Weed detection	CNN (AlexNet, VGG16, VGG19, ResNet50/101)	Groundnut weed dataset (24,816 images) & corn weed dataset	ResNet101 achieved -100% accuracy	Focus on weed detection, not sugarcane
Veeragandham & Santhi [34]	Multi-crop classification	Transfer learning with AgriNet (VGG16, VGG19, Inception-v3, InceptionResNet-v2, Xception)	AgriNet (160k agricultural images, 423 classes)	AgriNet-VGG19 achieved 94% accuracy	Domain-wide, not crop-specific maturity
Knott *et al.* [31]	Fruit grading (apple, banana)	Vision Transformer (pretrained)	Apple & banana datasets	Achieved competitive accuracy, 3× fewer samples	Not applied to sugarcane
Shah *et al.* [40]	Rice disease detection	Transfer learning (InceptionV3, VGG16, VGG19, ResNet50)	Rice leaf dataset (2000 images)	ResNet50 achieved 99.75% accuracy	Crop-specific, not sugarcane

Authors	Crop / Focus	Methodology	Dataset	Key Findings	Limitation / Gap
Daphal & Koli [32]	Sugarcane leaf disease	Transfer learning (MobileNetV2) + Ensemble	Self-created sugarcane leaf dataset (2569 images, five classes)	Ensemble reached 86.53% accuracy	Focus on leaf disease, not stalk quality
Sridhara *et al.* [27]	Sugarcane yield prediction	RF, SVM, SMLR, ANN	Indian sugarcane field data	ANN had the best prediction accuracy (R^2 higher, lower RMSE)	Focused on yield, not stalk Brix
Daphal & Koli [33]	Sugarcane disease detection	Attention-based CNN (AMRCNN)	Custom sugarcane leaf dataset	Outperformed VGG19, ResNet50, EfficientNet_B7 (86.53% accuracy)	Disease detection, not internode Brix
Ethiraj & Paranjothi [15]	Crop disease prediction	DenseNet-SVM + LIME (explainable AI)	Custom dataset	Achieved high interpretability and precision	Disease detection, not sugarcane Brix
Ruwanpathirana *et al.* [12]	Sugarcane growth monitoring	UAV RGB + ML (RF, MLR)	UAV images, DJI Mavic Pro	RF with CSM_PH + GLI achieved R^2=0.90	Focused on growth, not post-harvest quality
de França e Silva *et al.* [35]	Sugarcane yield estimation (review)	Remote sensing + simulation models	72 studies reviewed (2017–2023)	Remote sensing + models promising for yield	No focus on internode quality
Vasconcelos *et al.* [18]	Sugarcane yield prediction	Gamma regression, RF, ANN	Satellite-derived vegetation indices	Gamma regression achieved R^2=0.89	Focused on yield, not sugarcane Brix
Trivedi *et al.* [41]	Potato disease detection	CNN (VGG16, ResNet50) + Ensemble	Potato leaf dataset (2152 images)	Ensemble achieved 98.22% accuracy	Not related to sugarcane

[a] CNN = Convolutional Neural Network; RF = Random Forest; SVM = Support Vector Machine; ANN = Artificial Neural Network; SMLR = Stepwise Multiple Linear Regression; UAV = Unmanned Aerial Vehicle; DA = Domain Adaptation; DCGAN = Deep Convolutional Generative Adversarial Network; DNN = Deep Neural Network; mAP = mean Average Precision; RMSE = Root Mean Square Error; MLR = Multiple Linear Regression; YOLO = You Only Look Once (object detection framework); R-CNN = Region-based Convolutional Neural Network; LIME = Local Interpretable Model-agnostic Explanations; CSM_PH = Crop Surface Model Plant Height; GLI, VARI, GRVI, MGRVI = Vegetation Indices

2. Method

2.1. Methodological Framework

The proposed methodology establishes a non-destructive, image-based framework for classifying sugarcane internodes according to their Brix values. To address the lack of a standardized dataset for internode-level quality assessment, this study developed a new image dataset derived from two imaging configurations: Luar1 (single-internode photography) and Luar2 (internode split longitudinally). Each configuration was captured under both white and black backgrounds. This process resulted in four dataset categories: Luar1_Putih, Luar1_Hitam, Luar2_Putih, and Luar2_Hitam (Fig. 1). These configurations were designed to capture variation in surface texture, color, and morphology that may correlate with Brix levels, while also enabling an examination of how imaging setup and background influence classification performance. The deep learning framework enhances this dataset by preprocessing and augmenting the data, and by leveraging pre-trained convolutional neural networks for transfer learning. The aim is to develop a dependable, non-invasive technique for differentiating between higher- and lower-Brix internodes, which indicate sugarcane quality. The workflow follows a systematic

pipeline comprising dataset preparation, preprocessing, training, evaluation, and testing. Each stage is designed to improve model generalization and address challenges posed by imbalanced class distributions, which are frequently encountered in agricultural imaging.

Fig. 1. Sugarcane internode image categories: Luar1_Putih, Luar1_Hitam, Luar2_Putih, and Luar2_Hitam

The workflow is shown in Fig. 2. It begins with image acquisition and directory structuring, then preprocessing, such as resizing images to 224 × 224 pixels for CNN input. Data augmentation with controlled rotations, flipping, translation, zooming, and color jitter increases visual variability and reduces overfitting. The dataset is divided into training, validation, and testing subsets for performance assessment.

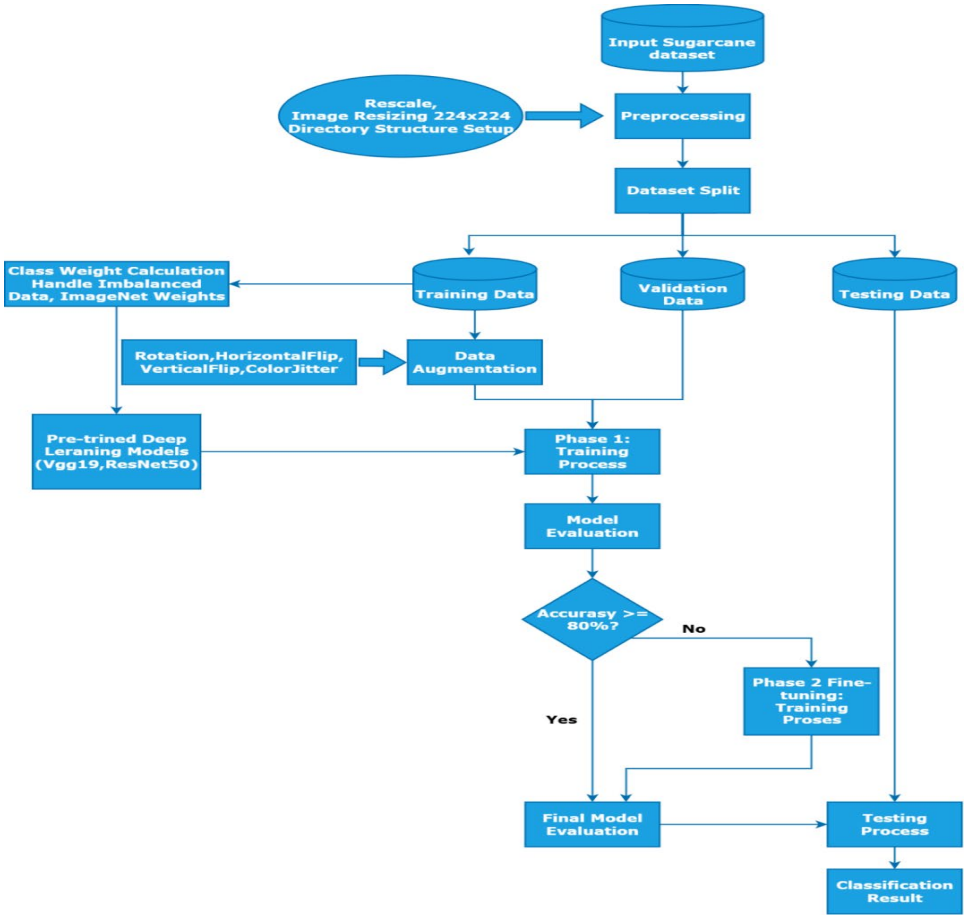

Fig. 2. A flowchart of methodology

To address class imbalance, class weights are used in training. Transfer learning applies to VGG19 and ResNet50. Training has two phases: initial learning and fine-tuning if validation accuracy does not reach 80 percent. Final evaluation uses the test set to complete the pipeline from image to quality prediction.

2.2. Data Collection

The study examines Bululawang sugarcane (*Saccharum officinarum* L.), widely grown in East Java and a principal raw material for white crystal sugar production at a national sugar company in Malang. Known for high yield and favorable sucrose content [42], post-harvest internodes (the segments between two nodes, or joints, on the sugarcane stalk) were collected, and their Brix levels, an indicator of dissolved sugar concentration, were assessed using a 0–32° Brix refractometer, capable of manual and automatic calibration for juice-based evaluation.

A total of 100 sugarcane stalks were harvested from the field. Each stalk was segmented into multiple internodes, except for the lowest three internodes, which were excluded because they are typically immature and not used for milling in industrial practice. For each remaining internode, its position along the stalk was recorded, and two external surface images (Luar1 and Luar2) were acquired to represent different sides of the same internode. These internodes were subsequently photographed under both white and black background configurations, producing four imaging categories: Luar1_Putih, Luar1_Hitam, Luar2_Putih, and Luar2_Hitam, as illustrated in Fig. 1.

Each image was labeled into one of two quality classes based on its measured Brix value: Brix A for values below 16 degrees Brix and Brix B for values equal to or above this threshold. This cutoff reflects the operational milling standard used by the collaborating sugar mill, which considers cane with Brix below 16 degrees unsuitable for processing. While widely applied, such thresholds may vary across regions or milling facilities.

Although Brix is inherently a continuous biochemical attribute that could be modeled using regression, the present work adopts a binary classification framework to align with the mill's categorical accept–reject decision process. This method guarantees practical applicability and mitigates the risk of overfitting to minor variations in Brix measurements, particularly considering the limited dataset size. Regression-based and multi-class formulations are acknowledged as promising directions for future research and are discussed in the Limitations and future work section.

All images were taken with a Samsung A13 smartphone featuring a 50-megapixel sensor and an f/1.8 aperture, utilizing 20-watt artificial lighting. The use of a smartphone camera was intended to emulate realistic field conditions and ensure practicality for potential farmer-oriented deployment.

To prevent data leakage and ensure independence across subsets, the dataset was partitioned at the internode level rather than at the individual image level. All images belonging to the same internode, including its Luar1 and Luar2 views under both background settings, were assigned to the same subset. Internodes were subsequently randomly assigned to training, validation, and test subsets with a predetermined random seed, with approximate proportions of 70%, 17%, and 13%, respectively. The distribution of internodes and images per class and per subset is presented in Table 2.

Table 2. Dataset distribution after preprocessing

Category	Brix class	Training	Validation	Testing	Total	Percentage split (Train/Val/Test)
Luar1_Putih	Brix A	568	143	88	799	71.1% / 17.9% / 11.0%
	Brix B	775	195	120	1,090	71.1% / 17.9% / 11.0%
Luar1_Hitam	Brix A	454	114	88	656	69.2% / 17.4% / 11.0%
	Brix B	624	156	120	900	69.3% / 17.3% / 13.3%
Luar2_Putih	Brix A	454	114	88	656	69.2% / 17.4% / 13.4%
	Brix B	620	155	120	895	69.3% / 17.3% / 13.4%
Luar2_Hitam	Brix A	571	145	88	804	71.1% / 18.0% / 10.9%
	Brix B	779	197	120	1,096	71.1% / 18.0% / 10.9%

In total, 100 sugarcane stalks were harvested from the field, and each stalk was cut into multiple internodes (ruas). The lowest three internodes near the stalk base were discarded because they are typically immature and not used for milling at the collaborating sugar mill. For each remaining

internode, we recorded its position along the stalk and then acquired two external surface images (Luar1 and Luar2) from opposite sides of the same internode.

To construct a deep learning classification dataset, images of each sugarcane internode were obtained by photographing the samples under different conditions, as illustrated in Fig. 1. The dataset comprises four categories: Luar1_Putih, Luar2_Putih, Luar1_Hitam, and Luar2_Hitam, representing different imaging perspectives and background conditions.

To prevent data leakage and maintain independence among the training, validation, and test sets, we partitioned the dataset at the internode level instead of the individual-image level. Concretely, each internode is treated as a single unit (sample), and all images derived from that internode (e.g., Luar1 and Luar2 captured on different sides and backgrounds) are assigned to the same subset. Internodes were subsequently randomly allocated to training, validation, and test sets using a predetermined random seed, with average proportions of 70%, 17%, and 13%, respectively. As a result, no internode contributes images to more than one subset, and the performance reported on the test set reflects generalization to previously unseen internodes. The corresponding numbers of internodes and images for each class and subset are summarized in Table 2.

2.3. Data Preprocessing

Data preprocessing was conducted to standardize and enhance the dataset before training the deep learning models. Since the collected images were obtained under varying illumination conditions and background settings, preprocessing was applied uniformly across all samples to improve the stability and reliability of model training. No cropping was used to preserve the original spatial context and structural characteristics of the sugarcane internodes, which may contain relevant visual cues related to Brix variation.

All images were downsized to a uniform resolution of 224 × 224 pixels, aligning with the standard input dimensions for convolutional neural network (CNN) architectures, including VGG19 and ResNet50. Pixel intensity values were then normalized using standard (z-score) normalization, defined as:

$$Normalized_{pixel} = \frac{(pixel - mean)}{std} \quad (1)$$

where pixel denotes the original intensity value, mean is the average pixel intensity of the dataset, and std is the corresponding standard deviation. This transformation centers the distribution around zero with unit variance, reduces illumination-related bias, accelerates training convergence, and enables the models to focus more effectively on discriminative visual features.

To further enhance model robustness, data augmentation techniques were applied during training, including arbitrary rotation, horizontal and vertical flipping, zooming, and luminance modification. These transformations simulate realistic variability in field conditions and help mitigate the effects of class imbalance, therefore enhancing the model's capacity to generalize to novel samples. The full augmentation specification is described in Section 2.4.

2.4. Model Training and Evaluation

This study employed a hold-out validation technique for model training. As described in Section 2.2, the dataset was partitioned into training, validation, and testing subsets at the internode level to ensure independence and avert data leakage. The training subset was used to optimize model parameters, the validation subset to monitor generalization and guide hyperparameter tuning, and the test subset to provide an unbiased assessment of model performance on unseen samples.

To address the moderate imbalance between the Brix A and Brix B classes, we used a class-weighted binary cross-entropy loss. A balanced strategy was adopted, with the weight assigned to each class inversely proportional to its frequency in the training subset. For example, if the training subset contained 150 images of Brix A and 450 photos of Brix B, the minority class, Brix A, received a weight of 2.0, and Brix B received approximately 0.67. During training, the per-sample binary cross-entropy

loss was multiplied by the corresponding class weight before averaging across the mini-batch. This weighting scheme was applied consistently to both VGG19 and ResNet50 across all imaging configurations.

Transfer learning was applied by initializing both networks with ImageNet weights to leverage generic visual feature representations. The training procedure consisted of two phases. In Phase 1, all convolutional layers of the pretrained backbone were kept frozen, while only the classification head, comprising the global average pooling layer, fully connected layers, and the final output layer, was trained. If stable convergence was achieved on the validation subset, the Phase 1 model proceeded directly to final testing. If not, Phase 2 was conducted by partially unfreezing deeper layers of the backbone and continuing training with a smaller learning rate. For VGG19, the convolutional layers in the last two convolutional blocks (Conv4_x and Conv5_x) were unfrozen, while Conv1_x through Conv3_x remained frozen. For ResNet50, the final residual stage (layer4 in PyTorch) was unfrozen, consisting of all convolutional and batch normalization layers in that stage, while conv1, bn1, layer1, layer2, and layer3 remained frozen. This selective unfreezing allowed both models to adapt high-level feature representations to the characteristics of the sugarcane internode images while limiting the number of trainable parameters and reducing the risk of overfitting.

In this application-oriented study, we did not conduct formal hypothesis testing, such as McNemar's test or repeated run t-tests, to compare the two models. Accordingly, the noted disparities in accuracy, precision, recall, and F1 score between VGG19 and ResNet50 are regarded as descriptive metrics of relative performance rather than statistically confirmed superiority. The absence of formal significance testing and the limited number of repeated training runs are acknowledged as methodological limitations and identified as opportunities for more rigorous evaluation in future work.

The final evaluation used the test subset to assess generalization performance and compare VGG19 and ResNet50 in terms of accuracy, robustness, and practical suitability for non-destructive sugarcane quality classification.

2.5. Data Augmentation

Augmentation was used to enhance the robustness of the classification models and mitigate overfitting. This step is crucial in agricultural imaging tasks, where variations in lighting, orientation, and camera positioning naturally occur during field acquisition. By introducing controlled transformations, the models are encouraged to generalize more effectively to unseen samples.

During training, the dataset was expanded on the fly using a combination of geometric and photometric transformations, as summarized in Table 3. Geometric augmentation consisted of random rotations within 15 degrees, horizontal and vertical translations up to 15 percent of the image dimensions, isotropic zooming between 0.85 and 1.15 times the original scale, and optional horizontal and vertical flipping. Photometric augmentation was implemented using color jitter with brightness, contrast, and saturation variations of up to 20 percent, and a hue shift of up to 0.1 in normalized HSV space, corresponding to approximately 36 degrees on the hue wheel. These operations were implemented using the RandomAffine and ColorJitter modules in PyTorch and were applied only to the training subset.

Table 3. Data augmentation parameters

Augmentation type	Parameters
Rotation	±15°
Width shifting	±15% of image width
Height shifting	±15% of image height
Zoom range	85% – 115%
Shearing	Not applied
Fill mode	Not applied

To enhance the robustness of the classification models and mitigate overfitting, data augmentation was applied. Augmentation is significant for agricultural imaging tasks, where natural variability in

lighting, angles, and positioning can influence image acquisition. By artificially expanding the dataset through controlled transformations, the models are encouraged to generalize better to unseen field conditions.

2.6. Model Selection

CNNs are widely used in image classification tasks, including agricultural imaging, where non-destructive quality assessment is essential. In this study, two representative architectures, VGG19 and ResNet50, were selected due to their complementary design principles and well-established performance in transfer learning applications. VGG19 follows a sequential architecture composed of stacked convolutional layers with uniform kernel sizes interleaved with max pooling operations. Its strength lies in its hierarchical feature extraction and architectural simplicity, which make it a reliable baseline for agricultural image classification. However, the large number of parameters requires substantial computational resources, resulting in increased training time and memory usage [43], [44]. ResNet50 incorporates residual connections that alleviate the vanishing gradient issue and facilitate the practical training of deeper networks. This design enhances accuracy and generalization, though it introduces greater architectural complexity and may require more careful hyperparameter tuning [45], [46].

Both models were initialized with ImageNet pretrained weights to exploit transfer learning. The classification heads were adapted to perform binary classification of internode images into Brix A (less than 16 degrees Brix) and Brix B (16 degrees Brix or higher). To ensure a fair comparison, identical preprocessing, augmentation, class weighting, and training strategies were applied to both architectures as described in Sections 2.3 through 2.5. The implementation details for each model are presented in Fig. 3 and Fig. 4 as pseudocode for reproducibility.

Pseudocode 1. VGG19 Training Framework

```
FUNCTION VGG19_Architecture():
INPUT: image of size 224×224×3
// Block 1
conv1_1 = CONV2D(64, 3×3, same, ReLU)
conv1_2 = CONV2D(64, 3×3, same, ReLU)
pool1 = MAXPOOL2D(2×2, stride=2)
// Block 2
conv2_1 = CONV2D(128, 3×3, same, ReLU)
conv2_2 = CONV2D(128, 3×3, same, ReLU)
pool2 = MAXPOOL2D(2×2, stride=2)
// Block 3 (4 conv layers)
conv3_1 = CONV2D(256, 3×3, same, ReLU)
conv3_2 = CONV2D(256, 3×3, same, ReLU)
conv3_3 = CONV2D(256, 3×3, same, ReLU)
conv3_4 = CONV2D(256, 3×3, same, ReLU)
pool3 = MAXPOOL2D(2×2, stride=2)
// Block 4 (4 conv layers)
conv4_1 = CONV2D(512, 3×3, same, ReLU)
conv4_2 = CONV2D(512, 3×3, same, ReLU)
conv4_3 = CONV2D(512, 3×3, same, ReLU)
conv4_4 = CONV2D(512, 3×3, same, ReLU)
pool4 = MAXPOOL2D(2×2, stride=2)
// Block 5 (4 conv layers)
conv5_1 = CONV2D(512, 3×3, same, ReLU)
conv5_2 = CONV2D(512, 3×3, same, ReLU)
conv5_3 = CONV2D(512, 3×3, same, ReLU)
conv5_4 = CONV2D(512, 3×3, same, ReLU)
pool5 = MAXPOOL2D(2×2, stride=2)
// Classifier
flatten = FLATTEN()
fc1 = FULLY_CONNECTED(4096, ReLU)
dropout1 = DROPOUT(0.5)
fc2 = FULLY_CONNECTED(4096, ReLU)
dropout2 = DROPOUT(0.5)
fc3 = FULLY_CONNECTED(num_classes, Softmax)
RETURN fc3
END FUNCTION
FUNCTION Train_VGG19_TransferLearning():
learning_rate = 0.001
batch_size = 32
epochs = 20
optimizer = ADAM(lr=learning_rate, weight_decay=1e-4)
model = LOAD_PRETRAINED_VGG19(weights='ImageNet')
FREEZE_BACKBONE(model)
REPLACE_CLASSIFIER(model, num_classes=2)
FOR epoch IN 1 TO epochs:
TRAIN(model, training_data, augmentation)
val_accuracy = VALIDATE(model, validation_data)
IF val_accuracy ≥ 80%:
BREAK
ELSE:
UNFREEZE_LAYERS(model)
REDUCE_LR(optimizer)
CONTINUE TRAINING
END FOR
TEST(model, testing_data)
END FUNCTION
```

Fig. 3. VGG19 Training Framework

2.7. Experimental Environment

All experiments were performed on Google Colaboratory, a cloud-based platform offering access to GPU-accelerated computing resources. The computational environment used an NVIDIA Tesla T4 GPU with 15.0 GB of VRAM and 12.7 GB of system RAM, providing sufficient capacity for training deep convolutional neural networks on medium-scale image datasets. The use of Colab also enabled

seamless integration with Python-based machine learning libraries and facilitated an efficient workflow for model implementation and evaluation. The methodology was implemented in Python 3.10 within a Jupyter Notebook environment. TensorFlow (version 2.19.0) and Keras were used to support core deep learning operations, while scikit learn was used for evaluation metrics, including accuracy, precision, recall, and F1 score. Image preprocessing and augmentation were performed using OpenCV and Imgaug, and NumPy and Pandas were employed for data handling and manipulation. Visualization tasks, including training curves and confusion matrices, were generated using Matplotlib and Seaborn.

To ensure reproducibility, a fixed random seed was applied throughout the experiments, and all models were trained with pretrained ImageNet weights. The availability of GPU acceleration significantly reduced training time and enabled practical experimentation with both VGG19 and ResNet50.

Pseudocode 2. ResNet50 Training Framework

```
FUNCTION ResNet50_Architecture():
INPUT: image of size 224×224×3
// Initial convolution
conv1 = CONV2D(64, 7×7, stride=2, same)
bn1 = BATCH_NORM(conv1)
relu1 = RELU(bn1)
pool1 = MAXPOOL2D(3×3, stride=2, same)
// Stage 1: 3 blocks
x = BottleneckBlock(pool1, 64, stride=1) × 3
// Stage 2: 4 blocks
x = BottleneckBlock(x, 128, stride=2)
x = BottleneckBlock(x, 128, stride=1) × 3
// Stage 3: 6 blocks
x = BottleneckBlock(x, 256, stride=2)
x = BottleneckBlock(x, 256, stride=1) × 5
// Stage 4: 3 blocks
x = BottleneckBlock(x, 512, stride=2)
x = BottleneckBlock(x, 512, stride=1) × 2
// Global Average Pooling
gap = GLOBAL_AVERAGE_POOLING(x)
fc = FULLY_CONNECTED(gap, num_classes, Softmax)
RETURN fc
END FUNCTION
FUNCTION Train_ResNet50_TransferLearning():
  learning_rate = 0.001
  batch_size = 32
  epochs = 20
  optimizer = ADAM(lr=learning_rate, weight_decay=1e-4)
  model = LOAD_PRETRAINED_RESNET50(weights='ImageNet')
  FREEZE_BACKBONE(model)
  REPLACE_CLASSIFIER(model, num_classes=2)
  FOR epoch IN 1 TO epochs:
    TRAIN(model, training_data, augmentation, class_weights)
    val_accuracy = VALIDATE(model, validation_data)
    IF val_accuracy ≥ 80%:
      BREAK
    ELSE:
      UNFREEZE_DEEPER_LAYERS(model)
  REDUCE_LR(optimizer)
  CONTINUE TRAINING
  END FOR
TEST(model, testing_data)
END FUNCTION
```

Fig. 4. ResNet50 Training Framework

3. Results and Discussion

2.8. Overview of the Experimental Framework

The experimental framework in this study was designed to classify sugarcane internodes into two quality categories, Brix A (<16 Brix) and Brix B (≥16 Brix), using deep learning–based approaches. The workflow integrated preprocessing, augmentation, and transfer learning with pretrained convolutional neural network architectures, followed by a two-phase training strategy. In Phase 1, all backbone layers were immobilized, and solely the classification head was trained to guarantee stable convergence. In Phase 2, fine-tuning was performed by unfreezing selected deeper layers when the validation accuracy did not reach the predefined threshold of 80%. Class imbalance was addressed by incorporating class weights into the loss function, and ImageNet pretrained weights were used to initialize both VGG19 and ResNet50. The model's performance was evaluated on the validation subset, and the final assessment was conducted on the reserved test subset to assess generalization.

This framework provides a systematic, reproducible approach to classify sugarcane internode quality and demonstrates the potential of deep learning for non-destructive agricultural assessment. By enabling rapid categorization of stalks into Brix groups, the methodology provides a pragmatic substitute for laboratory-based measures and facilitates more efficient decision-making in sugar mills. These findings highlight the role of artificial intelligence in enhancing precision agriculture and augmenting productivity and sustainability in sugarcane cultivation. The subsequent sections delineate the experimental outcomes derived from VGG19 and ResNet50, followed by a comparative analysis of their classification performance (see Table 4).

3.2. Process Validation

Table 4 presents the classification performance of the VGG19 model across the four imaging configurations: Luar1_Putih, Luar1_Hitam, Luar2_Putih, and Luar2_Hitam. Each configuration was evaluated using two training phases: Phase 1 (50 epochs), Phase 2 (100 epochs), and fine-tuning. During Phase 1, validation accuracies ranged from 66.35% to 68.27%, indicating limited extraction of internode picture features. After fine-tuning in Phase 2, accuracies improved across all configurations, ranging from 72.12% to 75.96%. The Luar2_Putih configuration yielded the best performance, achieving 75.96% accuracy, 76.58% precision, with an F1-score of 75.16%. These findings indicate that displaying both outer surfaces of a split internode against a white background provides more explicit structural cues for VGG19.

Table 4. Results of the classification of sugarcane quality using VGG19

Class	Mean Accuracy (%)		Mean Precision (%)		Mean Recall (%)		F1-Score (%)	
	Phase 1	*Phase 2*	*Phase 1*	*Phase 2*	*Phase 1*	*Phase 2*	*Phase 1*	*Phase 2*
Luar1_Putih	66.35	73.56	70.61	73.37	66.35	73.56	66.17	73.32
Luar1_Hitam	66.83	72.12	66.69	73.10	66.83	72.12	65.34	70.66
Luar2_Putih	67.79	75.96	67.47	76.58	67.79	75.96	66.90	75.16
Luar2_Hitam	68.27	73.08	69.27	74.52	68.27	73.08	66.07	71.52

Fig. 5 shows the learning curves for VGG19 on the Luar2_Putih dataset. In Phase 1, the model achieved 67.79% accuracy, with modest precision and recall. After fine-tuning in Phase 2, accuracy increased to 75.96%, precision rose to 76.58%, and recall for the Brix B (≥16 °Brix) class reached 0.89, indicating improved ability to identify high-quality cane.

Luar2_Putih: Training validation accuracy (Phase-1)-50 Epochs

Luar2_Putih: Training validation loss (Phase-1)-50 Epocs

Luar2_Putih: Training validation accuracy (Phase-2)-100 Epochs

Luar2_Putih: Training validation loss (Phase-2)- 100 Epochs

Fig. 5. Performance of VGG19 during training and validation on the Luar2_Putih dataset

Fig. 6 presents the corresponding confusion matrix; 51 of 88 Brix A (<16 °Brix) samples (58%) and 107 of 120 Brix B samples (89%) were correctly classified. Although recall for Brix A remained moderate, these values indicate that VGG19 occasionally accepted low-Brix internodes as suitable cane, which in practice may reduce sugar recovery if such samples are processed. Nevertheless, VGG19 demonstrated relatively strong overall performance for the Luar2_Putih configuration, confirming its suitability for non-destructive internode assessment.

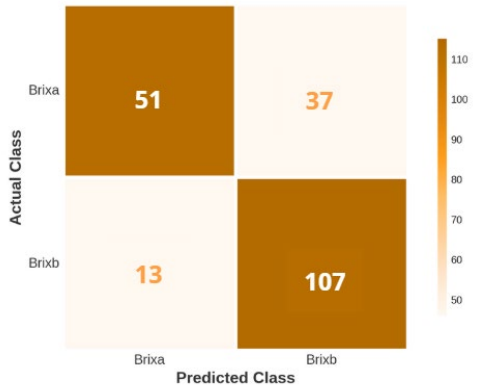

Fig. 6. Confusion matrix of the VGG19 for Luar2_Putih dataset

Table 5 presents the classification results of ResNet50 under the same four imaging configurations. The experimental results show that the optimal performance across all evaluation metrics was generally achieved in Phase 2. For Mean Accuracy, the highest value was achieved by the Luar2_Putih class at 78.85%, followed by Luar1_Putih at 75.96%, Luar1_Hitam at 73.08%, and Luar2_Hitam at 70.67%. In terms of Mean Precision, the optimal score was also recorded by Luar2_Putih at 81.04%, indicating the most precise classification among all classes, followed by Luar1_Putih (76.14%), Luar1_Hitam (73.76%), and Luar2_Hitam (70.63%). For Mean Recall, the best result again appeared in Luar2_Putih with 78.85%, while Luar1_Putih achieved 75.96%, Luar1_Hitam 73.08%, and Luar2_Hitam 70.67%. Similarly, the F1-Score, which balances precision and recall, reached its optimal value for Luar1_Putih at 76.02%, followed closely by Luar2_Putih (77.74%), Luar2_Hitam (70.65%), and Luar1_Hitam (71.94%), confirming that Phase 2 consistently produced improved and more balanced classification performance across the evaluated classes.

Table 5. Results of the classification of sugarcane quality using ResNet50

Class	Mean Accuracy (%)		Mean Precision (%)		Mean Recall (%)		F1-Score(%)	
	Phase 1	Phase 2	Phase 1	Phase 2	Phase 1	Phase 2	Phase 1	Phase 2
Luar1_Putih	68.27	75.96	67.97	76.14	68.27	75.96	67.46	76.02
Luar1_Hitam	71.63	73.08	71.52	73.76	71.63	73.08	71.56	71.94
Luar2_Putih	68.75	78.85	68.47	81.04	68.75	78.85	68.01	77.74
Luar2_Hitam	68.27	70.67	68.02	70.63	68.27	70.67	67.33	70.65

ResNet50 achieved higher accuracy and F1-scores than VGG19 in our experiments, particularly for Luar2_Putih, and Fig. 7 shows more stable training and validation behavior. Fine-tuning increased validation accuracy from 68.75% in Phase 1 to 78.85% in Phase 2, while validation loss steadily decreased.

Fig. 8 presents the confusion matrix; recall for Brix B reached 0.95, demonstrating strong performance on high-quality cane. Under the same Luar2_Putih conditions, ResNet50 achieved 78.85% accuracy, compared to VGG19's 75.96%, resulting in an improvement of approximately three percentage points. Because these values are derived from single-run experiments, this difference is interpreted as descriptive rather than statistically confirmed.

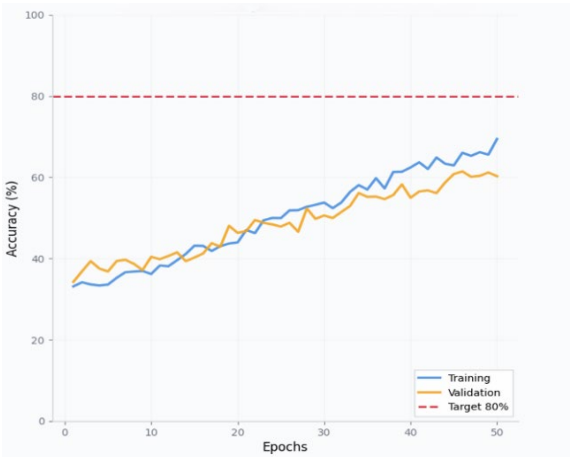

Luar2_Putih: Training validation accuracy (Phase-1)

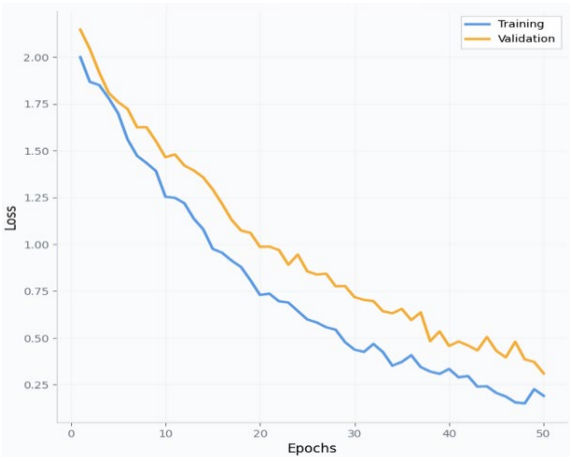

Luar2_Putih: Training validation loss (Phase-1)

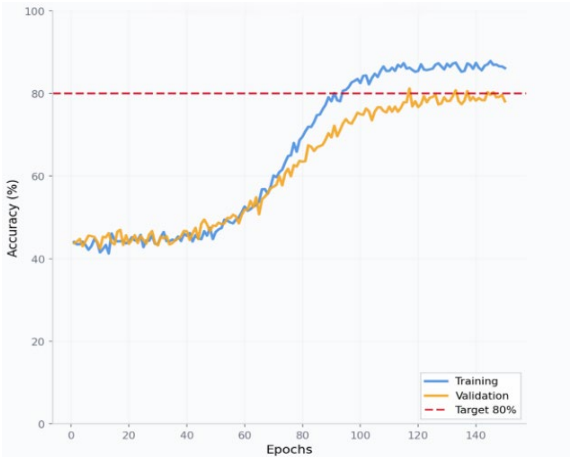

Luar2_Putih: Training validation accuracy (Phase-2) 100 Epochs

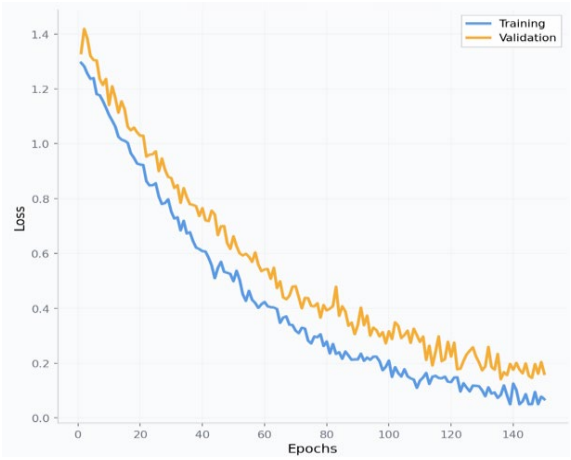

Luar2_Putih: Training validation loss (Phase-2)

Fig. 7. Performance of ResNet 50 during training and validation on the Luar2_Putih dataset

Although ResNet50 achieved higher overall accuracy, the improvement was moderate due to the dataset's characteristics. The distinction between <16 Brix and ≥16 Brix categories is based on subtle textural and color cues, which constrain the ability of deeper architectures to fully utilize their representational capacity. Additionally, both architectures were trained with identical preprocessing, augmentation, class weighting, and transfer-learning settings, which enabled a fair comparison while limiting divergence in their learned feature representations. These findings indicate that the proposed framework is stable, reliable, and not limited by methodological deficiencies.

Fig. 8 presents the confusion matrix for ResNet50 on the Luar2_Putih Phase 2 dataset, providing deeper insight into class-wise performance. Out of 88 Brix A samples, 50 were correctly classified (recall = 0.57), while 38 were misclassified as Brix B. For Brix B, the model achieved significantly stronger performance, correctly identifying 114 out of 120 samples (recall = 0.95) and misclassifying only six as Brix A. This distribution yields high precision for both classes (0.89 for Brix A and 0.75 for Brix B), demonstrating a more balanced trade-off compared to VGG19.

Beyond overall accuracy values, class-wise performance provides deeper insight into model behavior. ResNet50 consistently achieved higher recall and F1-scores for the Brix B class while maintaining comparable or slightly higher precision than VGG19. This suggests that ResNet50 is more effective at correctly identifying high-Brix internodes, which is operationally significant because misclassifying high-quality cane directly reduces potential mill yield. In contrast, VGG19 produced more false negatives for Brix B, resulting in lower recall despite similar accuracy in specific configurations.

These observations align with the architectural characteristics of the two backbones. ResNet50's deeper layers and residual connections facilitate the extraction of fine-grained textural cues, whereas VGG19's fully sequential design appears less responsive to subtle feature differences. Similar trends have been reported in the agricultural imaging literature, where deeper residual networks frequently outperform VGG-style models for fine-grained quality or disease classification tasks.

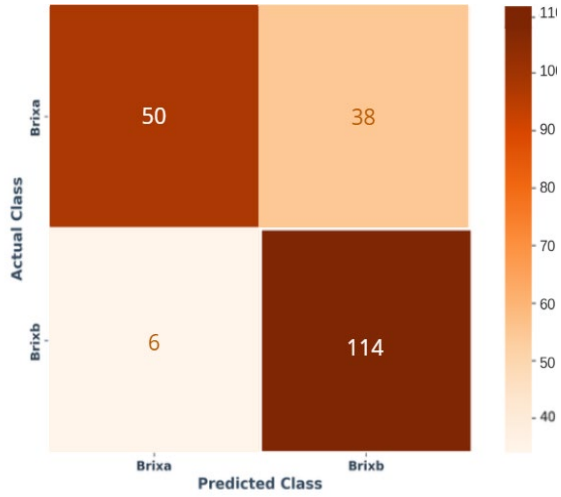

Fig. 8. Confusion matrix of the ResNet50

From a practical standpoint, the higher recall for Brix B achieved by ResNet50 indicates that this architecture is preferable in settings where avoiding missed high-Brix cane is prioritized, even when some borderline samples are occasionally classified as high quality. Although ResNet50 presented stronger descriptive performance patterns in this study, the absence of repeated runs and formal hypothesis testing means that these differences should be interpreted cautiously. Future research should incorporate multiple seeds and apply statistical tests such as McNemar's test to assess the significance of differences between architectures.

3.3. Managerial Insight

The findings of this study provide several practical and managerial insights for stakeholders across the sugarcane value chain. Across both VGG19 and ResNet50, the Luar2_Putih configuration yielded the strongest overall performance. This imaging setup, which places two adjacent internodes against a white background, is not only effective for deep learning models but also highly practical in field conditions. Farmers can easily reproduce this setup by cutting two consecutive internodes, positioning them side by side, and using a simple white surface such as HVS paper or cardboard. The simplicity of this protocol demonstrates that functional non-destructive assessment can be achieved using low-cost equipment, provided that imaging conditions are standardized.

From the farmer's perspective, early quality identification offers clear economic benefits. Determining whether internodes meet the ≥16 °Brix threshold before transporting cane to the mill helps avoid unnecessary transportation costs and reduces the likelihood of rejection. This promotes transparency and fairness in transactions, as decisions are based on objective, reproducible assessments rather than destructive testing or subjective evaluations.

For sugar mills, integrating AI-based classification into procurement workflows supports more accurate material planning, reduces fluctuations in sugar recovery, and enhances operational stability. A more consistent supply of high-Brix cane minimizes inefficiencies caused by quality variability and helps streamline scheduling and inventory management.

The confusion matrix analysis offers deeper insight into these operational trade-offs. For VGG19 under the Luar2_Putih configuration, the recall for Brix A (<16 °Brix) was 0.58, meaning that 42 percent of low-quality internodes were misclassified as suitable. Although this may benefit farmers in the short

term, mills could experience reduced sugar recovery when low-Brix cane enters the processing line. Conversely, the model correctly identified 0.89 of the high-Brix internodes (Brix B ≥ 16 °Brix), reducing potential income loss from wrongful rejection.

ResNet50 provided an even more favorable balance. While the recall for Brix A remained at 0.57, that for Brix B increased to 0.95, indicating that almost all suitable internodes were correctly identified. This reduces the risk of rejecting high-quality cane, benefiting farmers while ensuring that mills receive more consistent raw material.

Taken together, insights from Section 3.2 and the managerial analysis indicate that ResNet50 tended to produce higher descriptive performance and a more advantageous balance between recall and precision for the high Brix class. However, because the experiments were conducted using single runs without statistical significance testing, these differences should be interpreted as indicative rather than definitive. Moreover, even the best configuration, with an accuracy of 78.85 percent, implies that approximately one in five internodes is misclassified. Thus, the proposed models should be viewed as realistic baselines under field conditions rather than fully reliable autonomous solutions. The findings further highlight the inherent difficulty of inferring an internal biochemical property such as Brix from surface-level RGB imagery alone.

In summary, both models confirm that Luar2_Putih is the optimal imaging configuration, underscoring the value of standardized acquisition protocols. While ResNet50 showed stronger descriptive performance, the overall framework demonstrates that practical imaging procedures, combined with robust transfer learning, may offer valuable non-destructive decision-making assistance for sugar mills. This approach contributes to operational efficiency, fairer farmer–mill interactions, and long-term sustainability in the sugarcane supply chain.

3.4. Implications for SDGs

The findings of this study also support the achievement of multiple United Nations Sustainable Development Goals (SDGs). By enabling a non-destructive, low-cost, and scalable approach for sugarcane quality assessment, the proposed framework supports more sustainable and efficient practices across the agricultural value chain. Specifically, reducing waste generated by destructive laboratory testing and promoting more efficient use of agricultural resources align with Sustainable Development Goal 12. (Responsible Consumption and Production). By allowing farmers to classify internode quality before delivery, the framework also supports SDG 2 (Zero Hunger) by improving resource use, reducing losses, and enhancing income stability, thereby contributing to food system resilience.

Furthermore, the integration of artificial intelligence into quality control practices aligns with SDG 9 (Industry, Innovation, and Infrastructure), demonstrating the potential of digital innovation to modernize conventional agro-industrial systems and enhance their competitiveness. Reducing unnecessary cane transport and improving processing efficiency may also indirectly contribute to SDG 13 (Climate Action) by reducing energy use and emissions.

At a broader systems level, these implications highlight how AI-based solutions in agriculture can create multidimensional value, enhancing economic outcomes while simultaneously promoting sustainability, equity, and technological empowerment within the sugarcane ecosystem.

3.5. Empirical Contributions and Domain-Specific Implications

The empirical results of this study enhance comprehension of how deep learning models interpret internode-level visual cues for sugarcane quality assessment. While the Introduction has identified the absence of reproducible baselines for RGB-based Brix classification, the results presented in Section 3 demonstrate how this study addresses that gap in practice. Both VGG19 and ResNet50 achieved their highest performance under the Luar2_Putih imaging configuration, indicating that photographing two adjacent internodes against a white background provides the most informative structural and textural features for distinguishing between low- and high-Brix categories. This confirms that standardized and controlled imaging protocols play a central role in enabling reliable performance in non-destructive quality assessment.

Beyond the accuracy values, the confusion matrices for both models offer essential insights into operational outcomes. ResNet50 achieved a higher recall for the high-Brix class, which is economically significant because misclassifying high-quality cane as low-quality directly reduces potential yield and may impact farmer revenue. Conversely, both models showed more moderate recall for the low-Brix class, reflecting the intrinsic difficulty of detecting subtle textural differences associated with low sucrose content. These patterns illustrate the practical trade-offs inherent in deploying deep learning for field-level quality assessment and provide a quantified baseline against which future architectures can be evaluated.

The results also contribute conceptually to understanding how CNNs respond to internode-level imagery. The performance gap between VGG19 and ResNet50—although moderate—indicates that deeper residual architectures are better able to extract and refine mid-level patterns associated with Brix content. This suggests that future research should consider architectures designed to emphasize fine-grained texture representation or multimodal fusion with complementary sensors. Finally, the findings reinforce the relevance of AI-driven quality assessment to broader sustainability objectives. By reducing dependence on destructive laboratory testing and enabling more efficient use of harvested cane, AI-assisted classification aligns with sustainability priorities in agricultural value chains and supports efficient, transparent decision-making for both farmers and mills.

3.6. Limitations and future work

This study has several limitations that should be considered when interpreting its findings. First, the dataset consists of RGB images of a single sugarcane variety (Bululawang) collected under specific field conditions, which may restrict the applicability of the trained models to alternative varieties, seasons, or regions. While augmentation did enhance variability, the dataset's effective diversity remains modest.

Second, the study evaluated only two well-known CNN backbones, VGG19 and ResNet50, and each configuration was trained once without repeated runs using different random seeds or formal statistical significance testing. As a result, the observed performance differences should be interpreted as descriptive patterns rather than statistically validated superiority.

Third, the present work adopts a binary classification formulation based on the operational threshold of 16 °Brix used by the collaborating sugar mill. While this reflects current industrial practice, it limits flexibility for contexts where mills may use different or dynamic thresholds. A regression-based formulation that predicts continuous Brix values would provide richer information and greater adaptability, although such a model may require larger datasets to avoid overfitting.

From a performance standpoint, the best model (ResNet50 under Luar2_Putih) achieved an accuracy of 78.85 percent. This implies that approximately one in five internodes remains misclassified, confirming that the current model should be regarded as an initial, realistic baseline under field conditions rather than a definitive or state-of-the-art solution.

Future research can address these limitations in several directions. On the data side, collecting larger and more diverse datasets across multiple varieties, seasons, and geographical regions would enable more robust model training and facilitate studies on domain adaptation. Integrating supplementary sensing modalities, such as multispectral or hyperspectral imaging, could prove beneficial in capturing biochemical differences that are difficult to infer from RGB surface appearance.

On the modeling side, exploring lightweight architectures for mobile deployment (e.g., MobileNet or EfficientNet-Lite), more recent state-of-the-art classifiers (e.g., EfficientNet or vision transformers), or multimodal fusion architectures is a promising direction. Extending the task to regression-based prediction of Brix values or multi-class maturity levels could further enhance applicability.

Finally, real-time deployment scenarios should be evaluated, including inference speed on edge devices, user interface design for field operators, and integration with harvesting or milling workflows to quantify operational benefits. This study, therefore, provides a quantitative lower bound and a well-

defined starting point for future intelligent informatics systems for non-destructive sugarcane quality assessment.

4. Conclusion

This study evaluated the performance of two widely used convolutional neural network architectures, VGG19 and ResNet50, for non-destructive classification of sugarcane internodes into Brix A (<16 °C Brix) and Brix B (≥16 °C Brix) categories. Across all imaging configurations, fine-tuning consistently improved performance, with accuracies increasing from Phase 1 (50 epochs) to Phase 2 (100 epochs). Among all setups, the Luar2_Putih configuration yielded the strongest results for both architectures, indicating that photographing two adjacent internodes against a white background provides more explicit structural cues for Brix-based classification.

In our experiments, VGG19 achieved a maximum test accuracy of 75.96 percent, while ResNet50 reached 78.85 percent under the same configuration. Although these differences represent descriptive rather than statistically validated improvements, ResNet50 showed a more favorable balance of precision and recall, particularly for the high-Brix class. Confusion matrix analysis further showed that ResNet50 reduced the misclassification of high-quality cane, suggesting potential benefits for farmer income stability and improved operational efficiency at sugar mills. These findings highlight both the value and the difficulty of predicting an internal biochemical attribute using surface-level RGB information and emphasize the importance of establishing a well-characterized baseline for future intelligent informatics research.

Looking ahead, the proposed framework should be regarded as an initial feasibility baseline under field conditions. Future research may incorporate larger, more diverse datasets, integrate additional sensing modalities, such as multispectral or hyperspectral imaging, evaluate lightweight or more advanced architectures for mobile deployment, and explore regression-based prediction of continuous Brix values. The development of mobile or edge computing applications represents a promising direction for enabling real-time, low-cost assessment of sugarcane quality in field environments.

Such advancements have the potential to support progress toward several United Nations Sustainable Development Goals, encompassing SDG 2 (Zero Hunger), SDG 9 (Industry, Innovation, and Infrastructure), and SDG 12 (Responsible Consumption and Production). By reducing waste from destructive testing, improving resource efficiency, and enhancing transparency within agricultural value chains, AI-driven quality assessment can contribute to a more sustainable, resilient, and data-informed sugarcane industry.

Acknowledgment

This study was supported by the Ministry of Education, Science, and Technology through the Fundamental Research Grant and the Inter-University Collaborative Research Program 2025, Contract No. 503/UN62.21/PG.00.01/2025. The authors also gratefully acknowledge Universitas Pembangunan Nasional Veteran Yogyakarta for the institutional support and research facilities furnished throughout the study. In addition, the authors sincerely thank the editor and anonymous reviewers for their valuable comments and constructive suggestions, which have greatly enhanced the quality of this manuscript.

Declarations

Author contribution. N.I. and R.A.C.L. participated in the conceptual development, data management, and methodological design of the study. N.I. and R.A.C.L. conducted the investigation, with resources and data collection supplied by N.I. and P.M. H.C.R. and A.F. contributed to data labeling. H.C.R., A.F., and B.W. focused on software development and data processing. B.W. and R.A.C.L. handled visualization. The manuscript was collaboratively composed by N.I. and R.A.C.L. Project management and funding procurement were overseen by N.I. All authors have reviewed and authorized the final version of the manuscript for publication.

Funding statement. This research was funded by the Ministry of Education, Science, and Technology under grant No. 503/UN62.21/PG.00.01/2025.

Conflict of interest. The authors declare no conflict of interest.
Additional information. No additional information is available for this paper.

References

[1] OECD/FAO, "OECD-FAO Agricultural Outlook 2020-2029," Rome/OECD Publishing, Paris, 2020. doi: 10.1787/1112c23b-en.

[2] International Energy Agency, "Renewables 2021: Analysis and forecast to 2026," pp. 1- 175, 2021. [Online]. Available at: https://iea.blob.core.windows.net/assets/5ae32253-7409-4f9a-a91d-1493ffb9777a/Renewables2021-Analysisandforecastto2026.pdf.

[3] Republic of Indonesia, "Presidential Regulation No. 40 of 2023 on acceleration of national sugar self-sufficiency and provision of bioethanol as biofuel," pp. 1-14, 2023. [Online]. Available at: https://peraturan.bpk.go.id/Details/251973/perpres-no-40-tahun-2023.

[4] Climate Action Tracker, "Indonesia: Policies and action," 2024. [Online]. Available at: https://climateactiontracker.org/countries/indonesia/2024-12-10/policies-action/.

[5] United Nations, "Transforming our world: The 2030 Agenda for Sustainable Development," 2015. [Online]. Available at: https://sdgs.un.org/2030agenda.

[6] South African Sugarcane Research Institute, "Determining crop maturity for purposes of cane quality management (Information Sheet 4.7)," Mount Edgecombe, South Africa, pp. 1 - 6, 2022. [Online]. Available at: https://sasri.org.za/wp-content/uploads/2022/08/4.7-Determining-crop-maturity-for-purposes-of-cane-quality-management.pdf.

[7] V. Misra, A. K. Mall, S. Solomon, and M. I. Ansari, "Post-harvest biology and recent advances of storage technologies in sugarcane," *Biotechnology Reports*, vol. 33. p. e00850, 2022, doi: 10.1016/j.btre.2022.e00705.

[8] L. de P. Corrêdo, J. P. Molin, and R. Canal Filho, "Is It Possible to Measure the Quality of Sugarcane in Real-Time during Harvesting Using Onboard NIR Spectroscopy?," *AgriEngineering*, vol. 6, no. 1, pp. 64–80, 2024, doi: 10.3390/agriengineering6010005.

[9] C. Bisaglia *et al.*, "Machine Learning in Sustainable Agriculture: Systematic Review and Research Perspectives," *Agriculture*, vol. 15, no. 4, p. 377, 2025, doi: 10.3390/agriculture15040377.

[10] R. C. de Oliveira and R. D. de S. e. Silva, "Artificial Intelligence in Agriculture: Benefits, Challenges, and Trends," *Applied Sciences (Switzerland)*, vol. 13, no. 13. 2023, doi: 10.3390/app13137405.

[11] A. Sharma, A. Jain, P. Gupta, and V. Chowdary, "Machine Learning Applications for Precision Agriculture: A Comprehensive Review," *IEEE Access*, vol. 9, pp. 4843–4873, 2021, doi: 10.1109/ACCESS.2020.3048415.

[12] P. P. Ruwanpathirana *et al.*, "Evaluation of Sugarcane Crop Growth Monitoring Using Vegetation Indices Derived from RGB-Based UAV Images and Machine Learning Models," *Agronomy*, vol. 14, no. 9, p. 2059, Sep. 2024, doi: 10.3390/agronomy14092059.

[13] N. Amarasingam, F. Gonzalez, A. S. A. Salgadoe, J. Sandino, and K. Powell, "Detection of White Leaf Disease in Sugarcane Crops Using UAV-Derived RGB Imagery with Existing Deep Learning Models," *Remote Sens.*, vol. 14, no. 23, p. 6137, Dec. 2022, doi: 10.3390/rs14236137.

[14] Y. Huang, R. Li, X. Wei, Z. Wang, T. Ge, and X. Qiao, "Evaluating Data Augmentation Effects on the Recognition of Sugarcane Leaf Spot," *Agric.*, vol. 12, no. 12, 2022, doi: 10.3390/agriculture12121997.

[15] R. Pudupet Ethiraj and K. Paranjothi, "A deep learning-based approach for early detection of disease in sugarcane plants: an explainable artificial intelligence model," *IAES Int. J. Artif. Intell.*, vol. 13, no. 1, p. 974, Mar. 2024, doi: 10.11591/ijai.v13.i1.pp974-983.

[16] M. R. Barbosa Júnior, B. R. de A. Moreira, R. P. de Oliveira, L. S. Shiratsuchi, and R. P. da Silva, "UAV imagery data and machine learning: A driving merger for predictive analysis of qualitative yield in sugarcane," *Front. Plant Sci.*, vol. 14, pp. 1–11, Jan. 2023, doi: 10.3389/fpls.2023.1114852.

[17] T. F. Canata, M. C. F. Wei, L. F. Maldaner, and J. P. Molin, "Sugarcane Yield Mapping Using High-Resolution Imagery Data and Machine Learning Technique," *Remote Sens.*, vol. 13, no. 2, p. 232, Jan. 2021, doi: 10.3390/rs13020232.

[18] J. C. S. Vasconcelos, C. S. Arantes, E. A. Speranza, J. F. G. Antunes, L. A. F. Barbosa, and G. M. de A. Cançado, "Predicting Sugarcane Yield Through Temporal Analysis of Satellite Imagery During the Growth Phase," *Agronomy*, vol. 15, no. 4, p. 793, Mar. 2025, doi: 10.3390/agronomy15040793.

[19] S. Widodo, A. Ahmar, and M. Solahudin, "Nondestructive Prediction of Brix Value in Sugarcane Based of Portable NIR Spectroscopy," *J. Keteknikan Pertan.*, vol. 12, no. 3, pp. 424–437, Dec. 2024, doi: 10.19028/jtep.012.3.424-437.

[20] M. V. A. da Costa, C. H. Fontes, G. Carvalho, and E. C. de M. Júnior, "UltraBrix: A Device for Measuring the Soluble Solids Content in Sugarcane," *Sustainability*, vol. 13, no. 3, p. 1227, Jan. 2021, doi: 10.3390/su13031227.

[21] S. A. Jaywant, H. Singh, and K. M. Arif, "Sensors and Instruments for Brix Measurement: A Review," *Sensors*, vol. 22, no. 6, p. 2290, Mar. 2022, doi: 10.3390/s22062290.

[22] U. Nawaz, M. Z. Zaheer, F. S. Khan, H. Cholakkal, S. Khan, and R. M. Anwer, "AI in Agriculture: A Survey of Deep Learning Techniques for Crops, Fisheries and Livestock," *arXiv*, pp. 1–42, 2025, [Online]. Available at: https://arxiv.org/abs/2507.22101.

[23] F. Ali *et al.*, "From Sensors to Insights: The Fusion of AI, Edge Computing, and Precision Agriculture," *J. Agric. Biol.*, vol. 3, no. 1, pp. 160–170, Feb. 2025, doi: 10.55627/agribiol.003.01.1067.

[24] W. B. Demilie, "Plant disease detection and classification techniques: a comparative study of the performances," *J. Big Data*, vol. 11, no. 1, p. 5, Jan. 2024, doi: 10.1186/s40537-023-00863-9.

[25] H. M. Yusuf, S. A. Yusuf, A. H. Abubakar, M. Abdullahi, and I. H. Hassan, "A systematic review of deep learning techniques for rice disease recognition: Current trends and future directions," *Franklin Open*, vol. 8, no. July, p. 100154, Sep. 2024, doi: 10.1016/j.fraope.2024.100154.

[26] N. Ismail and O. A. Malik, "Real-time visual inspection system for grading fruits using computer vision and deep learning techniques," *Inf. Process. Agric.*, vol. 9, no. 1, pp. 24–37, Mar. 2022, doi: 10.1016/j.inpa.2021.01.005.

[27] S. Sridhara, Soumya B. R., And G. R. Kashyap, "Multistage sugarcane yield prediction using machine learning algorithms," *J. Agrometeorol.*, vol. 26, no. 1, pp. 37–44, Mar. 2024, doi: 10.54386/jam.v26i1.2411.

[28] P. M. Kai, B. M. de Oliveira, and R. M. da Costa, "Deep Learning-Based Method for Classification of Sugarcane Varieties," *Agronomy*, vol. 12, no. 11, p. 2722, Nov. 2022, doi: 10.3390/agronomy12112722.

[29] Z. Li, G. Chen, and T. Zhang, "A CNN-Transformer Hybrid Approach for Crop Classification Using Multitemporal Multisensor Images," *IEEE J. Sel. Top. Appl. Earth Obs. Remote Sens.*, vol. 13, pp. 847–858, 2020, doi: 10.1109/JSTARS.2020.2971763.

[30] T. Kattenborn, J. Leitloff, F. Schiefer, and S. Hinz, "Review on Convolutional Neural Networks (CNN) in vegetation remote sensing," *ISPRS J. Photogramm. Remote Sens.*, vol. 173, pp. 24–49, Mar. 2021, doi: 10.1016/j.isprsjprs.2020.12.010.

[31] M. Knott, F. Perez-Cruz, and T. Defraeye, "Facilitated machine learning for image-based fruit quality assessment," *J. Food Eng.*, vol. 345, p. 111401, May 2023, doi: 10.1016/j.jfoodeng.2022.111401.

[32] S. D. Daphal and S. M. Koli, "Enhancing sugarcane disease classification with ensemble deep learning: A comparative study with transfer learning techniques," *Heliyon*, vol. 9, no. 8, p. e18261, Aug. 2023, doi: 10.1016/j.heliyon.2023.e18261.

[33] S. D. Daphal and S. M. Koli, "Enhanced deep learning technique for sugarcane leaf disease classification and mobile application integration," *Heliyon*, vol. 10, no. 8, p. e29438, Apr. 2024, doi: 10.1016/j.heliyon.2024.e29438.

[34] S. Veeragandham and H. Santhi, "Effectiveness of convolutional layers in pre-trained models for classifying common weeds in groundnut and corn crops," *Comput. Electr. Eng.*, vol. 103, p. 108315, Oct. 2022, doi: 10.1016/j.compeleceng.2022.108315.

[35] N. R. de França e Silva, M. E. D. Chaves, A. C. dos S. Luciano, I. D. Sanches, C. M. de Almeida, and M. Adami, "Sugarcane Yield Estimation Using Satellite Remote Sensing Data in Empirical or Mechanistic Modeling: A Systematic Review," *Remote Sens.*, vol. 16, no. 5, p. 863, Feb. 2024, doi: 10.3390/rs16050863.

[36] E. C. Too, L. Yujian, S. Njuki, and L. Yingchun, "A comparative study of fine-tuning deep learning models for plant disease identification," *Comput. Electron. Agric.*, vol. 161, pp. 272–279, Jun. 2019, doi: 10.1016/j.compag.2018.03.032.

[37] J. Chen, J. Chen, D. Zhang, Y. Sun, and Y. A. Nanehkaran, "Using deep transfer learning for image-based plant disease identification," *Comput. Electron. Agric.*, vol. 173, p. 105393, Jun. 2020, doi: 10.1016/j.compag.2020.105393.

[38] W. Zhao, W. Yamada, T. Li, M. Digman, and T. Runge, "Augmenting Crop Detection for Precision Agriculture with Deep Visual Transfer Learning—A Case Study of Bale Detection," *Remote Sens.*, vol. 13, no. 1, p. 23, Dec. 2020, doi: 10.3390/rs13010023.

[39] P. Maheswari, P. Raja, and V. T. Hoang, "Intelligent yield estimation for tomato crop using SegNet with VGG19 architecture," *Sci. Rep.*, vol. 12, no. 1, p. 13601, Aug. 2022, doi: 10.1038/s41598-022-17840-6.

[40] S. R. Shah, S. Qadri, H. Bibi, S. M. W. Shah, M. I. Sharif, and F. Marinello, "Comparing Inception V3, VGG 16, VGG 19, CNN, and ResNet 50: A Case Study on Early Detection of a Rice Disease," *Agronomy*, vol. 13, no. 6, p. 1633, Jun. 2023, doi: 10.3390/agronomy13061633.

[41] A. K. Trivedi, T. Mahajan, T. Maheshwari, R. Mehta, and S. Tiwari, "Leveraging feature fusion ensemble of VGG16 and ResNet-50 for automated potato leaf abnormality detection in precision agriculture," *Soft Comput.*, vol. 29, no. 4, pp. 2263–2277, 2025, doi: 10.1007/s00500-025-10523-0.

[42] R. Yunita, R. S. Hartati, S. Suhesti, and Syafaruddin, "Response of bululawang sugarcane variety to salt stress," *IOP Conf. Ser. Earth Environ. Sci.*, vol. 418, no. 1, p. 012060, Jan. 2020, doi: 10.1088/1755-1315/418/1/012060.

[43] P. Johri *et al.*, "Advanced deep transfer learning techniques for efficient detection of cotton plant diseases," *Front. Plant Sci.*, vol. 15, p. 1441117, 2024, doi: 10.3389/fpls.2024.1441117.

[44] H. Ghosh *et al.*, "Advanced neural network architectures for tomato leaf disease diagnosis in precision agriculture," *Discov. Sustain.*, vol. 6, no. 1, p. 312, 2025, doi: 10.1007/s43621-025-01149-1.

[45] Y. Pamungkas, E. Triandini, W. Yunanto, and Y. Thwe, "Impact of Hyperparameter Tuning on ResNet-UNet Models for Enhanced Brain Tumor Segmentation in MRI Scans," *Int. J. Robot. Control Syst.*, vol. 5, no. 2, pp. 917–936, Mar. 2025, doi: 10.31763/ijrcs.v5i2.1802.

[46] T. Shi, J. Yu, Z. Hu, and K. Jiang, "Improved Method of ResNet50 Image Classification Based on Transfer Learning," *Int. J. Adv. Network, Monit. Control.*, vol. 10, no. 2, pp. 1–9, Jun. 2025, doi: 10.2478/ijanmc-2025-0011.